Achieving PeV-Scale Neutrino-Proton Collisions via Staggered Beamlines

Tome Anticic[a]

[a] *Ruder Boskovic Institute, Bijenicka 54, Zagreb, Croatia*

Abstract

This paper introduces a novel accelerator-based method to achieve neutrino-proton interactions at energies from 10 to 100 PeV in a controlled laboratory environment. By employing a staggered configuration of a pion decay tunnel and a proton beamline, the method effectively counters neutrino beam divergence, forming repeated overlaps between narrow neutrino beams and the proton beam. Simulations, using parameters from the Future Circular Collider and including muon cooling to enhance event rates, demonstrate the potential to generate hundreds to thousands of events annually at these ultra-high energies. While the proposed setup presents very significant technological challenges, it could potentially open a new energy range in neutrino physics, enabling precise measurements of neutrino-nucleon cross-sections needed for interpreting high-energy astrophysical neutrino signals and for testing fundamental physics.

Keywords: neutrinos, accelerators, FCC, muon cooling, PeV energy, staggered beams

1. Introduction

Precise measurements of neutrino-hadron interaction cross-sections in the PeV energy range and above are crucial for interpreting astrophysical neutrino signals such as those originating from active galactic nuclei, gamma-ray bursts, or evaporating primordial black holes [1, 2, 3, 4]. They can also provide insights into small-x QCD dynamics [5], or test the Standard Model in previously inaccessible energy domains [6, 7].

Neutrino-hadron interactions have been studied over a wide range of energies, but never in a controlled experiment beyond the ∼TeV scale. Conventional accelerator-based neutrino experiments produce neutrinos with energies up to a few hundred GeV via pion decay [8]. Recently, the FASERν experiment at the LHC observed neutrino interactions at energies of a few TeV [9].

Beyond this energy range, neutrino-hadron data come only from rare astrophysical events. The IceCube observatory, for example, has detected neutrinos with energies up to several PeV [10, 11, 12], while the KM3NeT neutrino telescope indirectly observed a neutrino of about 200 PeV [13]. In addition to the lack of controlled data, significant theoretical uncertainty exists in the cross-section at these energies [14, 15].

Currently, there are no laboratory sources of neutrinos above the ∼TeV scale, nor is there an experimental technique capable of generating neutrino-hadron collisions at the PeV energy scale or beyond. Simply increasing the energy of a traditional neutrino beamline is insufficient, as even a multi-TeV proton beam hitting a fixed target produces neutrinos only up to the hundreds-of-GeV scale. These neutrino beamlines pose additional significant challenges. While the charged pion parents can be focused to some extent with magnetic horns [16], the neutrinos themselves cannot be focused. As a result, the neutrino flux rapidly dilutes with distance from the source. This dispersion, combined with the need to compensate for the very low neutrino interaction probability, also necessitates massive, kiloton-scale detector volumes.

This paper explores a new collider-like approach that addresses these challenges, using relativistic kinematics and a novel staggered beamline configuration. One component of the novel approach is to collide a high-energy neutrino beam head-on with a high-energy proton beam, so that in the proton beams rest frame, the neutrinos lab-frame energy is Lorentz boosted. This boost can, in principle, transform relatively low lab-frame neutrino energies into the multi-PeV energy range. The second key component is arranging the pion decay tunnel and proton beamline in a repeating

Email address: `anticic@irb.hr` (Tome Anticic)

staggered pattern of short segments, so that each segment of the proton beamline is exposed to a narrow neutrino flux from the short segment of pions just ahead of the protons, as illustrated in Figure 1.

Simulations using parameters based on the Future Circular Collider (FCC-hh) [17] plans demonstrate the feasibility of this approach to yield detectable event rates and to possibly open a new frontier in high-energy physics.

Sections 2 and 3 describe the methodology and simulation setup used to evaluate the idea. Section 4 presents the simulation results, demonstrating the gain in event rates due to the staggered arrangement, as well as the achievable neutrino energies. Next, we discuss the implications of the results and the significant engineering challenges in Sections 5 and 6. Finally, we summarize our findings and the outlook for this concept in Section 7.

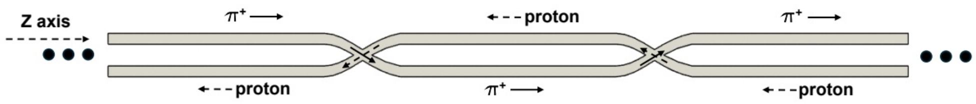

Figure 1: Proposed staggered arrangement illustrating periodic realignment of pion decay tunnels and proton beamlines.

2. Methodology

2.1. Kinematics

An important component of our proposed method is the use of relativistic kinematics to achieve higher neutrino-proton energies, cross-section enhancement, and larger neutrino fluxes. Specifically, if a neutrino with energy $E_{\nu,\mathrm{lab}}$ strikes a high-energy proton of energy E_p head-on, the neutrinos energy in the protons rest frame is boosted due to the relativistic Lorentz transformation and is approximately:

$$E_{\nu,\mathrm{rest}} \approx 2\gamma_p E_{\nu,\mathrm{lab}}, \tag{1}$$

where $\gamma_p = E_p/m_p$, and m_p is the proton mass. For example, a 100 GeV neutrino colliding with a 1 TeV proton results in $E_{\nu,\mathrm{rest}} \approx 200\,\mathrm{TeV}$, while for a 50 TeV proton, the same neutrino reaches $E_{\nu,\mathrm{rest}} \approx 10\,\mathrm{PeV}$.

If the neutrino beam itself extends to TeV-scale energies (which is possible from the decay of very high-energy pions), the effective collision energy can reach well into the hundreds of PeV. This increase in neutrino energy also directly translates into a larger deep-inelastic neutrino-proton cross-section [14], partially compensating for the low neutrino flux.

Another beneficial effect of high-energy pions is more collimated neutrino beams, since the neutrino angular spread in the lab frame with respect to the parent pion direction is $\approx 1/\gamma_\pi$, where $\gamma_\pi = E_\pi/m_\pi$. As a result, the proton beamline is exposed to larger neutrino fluxes than would be the case for the same number of pions at lower energies.

2.2. Staggered beamline configuration

The kinematic effects of higher energies are insufficient to offset the extremely low density of the proton beam. For example, at the LHC, the density of protons in the beamline is around 10^{14} protons per cubic meter, about 16 orders of magnitude lower than the nucleon density of solid matter (e.g., liquid argon has $\sim 8 \times 10^{29}$ nucleons/m^3).

This disparity is addressed to a large extent by our concept of a staggered alignment of the pion and proton beams (Figure 1). In this method the two beams are initially aligned along the z-axis and move in opposite directions. Both beams are at regular intervals deflected transversely with respect to the z-axis by a small distance in opposite directions and then realigned to continue along their respective paths but with a small transverse offset. This way a series of short sections is formed where the neutrino beam from the pion decay tunnel overlaps with the proton beamline.

In effect, the neutrino beam is continuously reset to a narrow transverse width at regular intervals along the full length of the proton beamline, rather than only at its start. This is in contrast to the standard single-pass setup, where the neutrino flux continuously decreases with distance as the beam diverges. The proposed method thus significantly increases the total neutrino-proton interaction probability over a long distance.

2.3. Neutrino production via pion decay

The pion beam is produced using established methods from neutrino factories [16], with a high-energy proton beam impinging on a target, and a magnetic horn selecting positively charged pions and collimating them. Focusing magnets along the pion decay tunnel further tighten the beam, and the decaying pions then produce a collimated muon neutrino beam in the forward direction.

2.4. Neutrino production via muon decay

In addition to ν_μ, each π^+ also decays to μ^+. These muons then decay via $\mu^+ \to e^+ + \nu_e + \bar{\nu}_\mu$, providing additional neutrinos to interact with the proton beam. The $\bar{\nu}_\mu$-proton charged-current deep-inelastic scattering interaction produces a μ^-, just as a ν_μ-proton interaction produces a μ^+, with similar cross-sections in the PeV range [14]. In our simulation, we considered only the events involving muon final states, as the electron showers from electron neutrino-proton interactions are much more challenging to detect.

At the TeV energy scale, the $2.2\,\mu$s muon lifetime results in decay lengths of thousands of kilometers, potentially enabling ionization cooling. In this process (demonstrated by the MICE collaboration [18]), muons pass through absorbers to lose energy, reducing the transverse and longitudinal emittance, followed by re-acceleration to restore longitudinal momentum. This technique, planned to be used in future muon colliders [19], would result in very low emittance muon beams, and thus in much narrower neutrino beams.

2.5. Integration with a synchrotron accelerator

Our method could be implemented in a future accelerator complex by modifying a proton synchrotron design, such as the FCC-hh. In this setup, one proton beamline serves as the neutrino interaction target, while the counter-rotating proton beamline is the source of protons diverted to a fixed target to create pions, as in conventional neutrino beams [16]. Two long straight sections are placed between the bending halves (see Figure 2), with the straight sections featuring the staggered arrangement of the pion decay tunnel and the proton beamline. Pions that do not decay in the first straight section are bent around the semicircle to repeat the process, further increasing the neutrino-proton interaction yield. This pattern repeats until most pions decay, utilizing the full pion decay length. The same method would also apply to both cooled and uncooled muons.

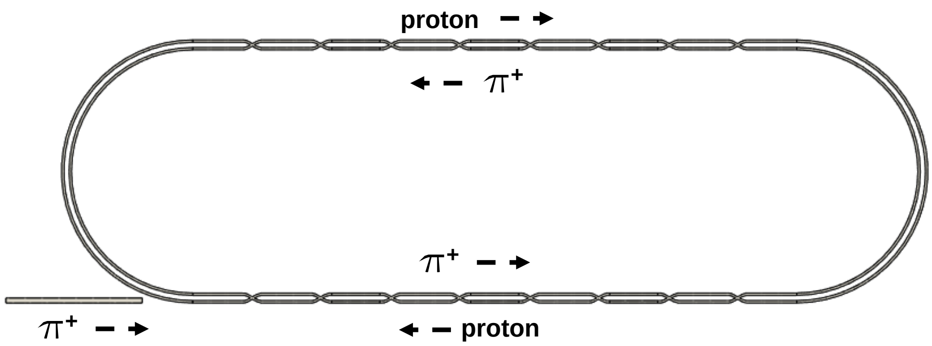

Figure 2: Schematic of the synchrotron setup with two staggered straight sections between bending arcs. Pions can circulate between sections if their decay length allows, enhancing interaction yield. The counter-rotating proton beamline is not shown.

3. Simulation

To assess the viability of the proposed staggered pion beam-proton beam collider, we developed a simplified Monte Carlo simulation of the pion decay and neutrino-proton interaction process. The simulation incorporates several idealizations, focusing on the impact of the staggered design on event rates and using parametric models for beam intensities.

The highest planned accelerator energies and rates are those envisaged for the FCC-hh Phase II [20, 17], and are thus used in our simulation. Hence, our simulation assumes a 50 TeV energy for both the protons in the proton beamline and the protons hitting the fixed target. The semicircle arc length of the accelerator setup in Figure 2 is 50 km, while the lengths of the long straight staggered sections are, somewhat arbitrarily, set to 200 km each (larger lengths yield higher rates). The staggered section lengths are set to 100 m. The pion beam was set to have a fixed spot size of RMS 1 mm throughout its path, chosen as an optimistic but potentially achievable target based on current technology projections (see Section 6). Unless otherwise stated, these parameters are the default in the various scenarios investigated in the simulations.

Pion production: Pythia 8.3 [21] was used to generate high-energy protons of constant energy hitting a fixed proton target, with positive pions selected from the produced secondaries. The pion transverse p_T and longitudinal p_l momenta were kept unchanged throughout the pion decay tunnel. This p_T, peaking at the Fermi momentum of around ~ 0.3 GeV, sets the angular divergence for the pions once they decay.

Pion beam: The pions are propagated in small dz steps along the tunnel path, with the decay length modelled stochastically.

Staggered design: The pions initially traverse a 1 km section in the $+z$ direction, representing a standard accelerator neutrino beam horn and decay tunnel. The pion beam is then staggered at fixed intervals, with perpendicular offsets moving the pion beam to and from the z-axis. The proton beam, with a momentum in the $-z$ direction, is also staggered, with each segment offset with respect to the pion beam segments (Figure 1). This staggered pattern is repeated throughout the two straight sections of the accelerator.

Proton beam: The proton beam is set to a fixed line density rather than being composed of individual bunches.

Neutrino production: When a pion decays, a neutrino is generated with an energy and angle relative to the pion direction according to isotropic two-body decay kinematics in the pion rest frame. The neutrinos direction with respect to the pion direction in the lab frame thus has an average angle of $1/\gamma_\pi$, with the pion itself already possessing an angle with respect to the horizontal direction of p_T/p_l. The neutrino is tracked in small dz steps along its path and is recorded if, at a distance z from the target, its transverse distance from the proton beamline is within 1 mm. This yields $\Phi_\nu(z, E'_\nu)$, the neutrino flux per proton on target (POT), where E'_ν is the neutrino energy in the proton rest frame.

Muon beam: As with the pions, the muon beam width was fixed to an RMS of 1 mm throughout the decay pipe. After a muon decays, a $\bar{\nu}_\mu$ is generated with an energy and angle relative to the muon direction according to isotropic three-body decay kinematics in the muon rest frame. The rest of the process is the same as for the neutrinos from pion decay. For the cooled muon beam, the beam width and transverse momenta were set to zero, so that the only contribution to the neutrino beam spread is the decay kinematics, with an average angle of $1/\gamma_\mu$, ($\gamma_\mu = E_\mu/m_\mu$) relative to the z-axis.

The total number of events per year is found by numerically integrating over the full path of the proton beamline:

$$N_{\text{events}}/\text{year} = (N_{\text{POT}}/\text{year}) \times \lambda_p \times \int \Phi_\nu(z, E'_\nu) \times \sigma_{\nu p}(E'_\nu)\, dz, \tag{2}$$

where $\sigma_{\nu p}(E'_\nu)$ is the neutrino-proton cross-section [14], $N_{\text{POT}}/\text{year}$ is the number of protons on target per year, and λ_p is the proton line density (protons per meter) in the beamline.

4. Results

The simulation results are presented per one POT/year and per one proton/m in the proton beamline. To find the expected number of events, both realistic (using planned FCC-hh parameters) and more optimistic or alternative scenarios for POT/year and protons/m are then used.

4.1. Viability of the staggered method

Figure 3 illustrates the effectiveness of the staggered method compared to the standard way of generating accelerator neutrinos. Three scenarios are shown, all of which have an initial 1 km decay tunnel and a proton beamline in front of it:

Staggered configuration: The pion beam first traverses the initial 1 km decay tunnel. Afterwards, both the proton beamline and the pion decay tunnel are staggered, in line with our proposed method. The pion beam width is set to a 1 mm RMS size throughout the decay tunnel.

Focused pion beam (non-staggered): Like above, the pion beam starts by remaining focused in the decay tunnel. However, at the end of the tunnel the beam dissapears, simulating a beam dump just before the proton beamline.

Conventional (non-staggered, no focusing of pion beam): The pion beam is unfocused in the decay tunnel, and thus diverges due to the pion transverse momenta set at the target. As in the previous case, at the end of the tunnel the beam gets dumped. This represents a typical accelerator neutrino beam configuration at high energy.

We plot the results for only the first km of the proton beamline to more clearly visualize the effects of the staggered method. In the conventional case (non-staggered, non-focused), the event rate falls off roughly exponentially with distance. The focused but non-staggered case has a similar exponential drop, but with a several times larger cumulative number of events due to the narrow pion beam forming a more concentrated neutrino beam. For both cases the event rates drop to effectively zero after only a kilometer along the proton beamline.

In contrast to the conventional and focused non-staggered cases, the staggered configuration maintains a high interaction rate by periodically resetting the neutrino beam's transverse width the proton beam is exposed to. In fact, by extending the simulation up to 2000 km (at which point most of the pions have decayed), we find the total neutrino-proton interaction count to be $\approx 2 \times 10^3$ times higher than the focused non-staggered case, and $\approx 10^4$ times larger than the conventional case.

4.2. Sensitivity to beam parameters

Figure 4 presents the dependence of the interaction rate on the staggered segment length on a log-log scale, demonstrating an inverse power relation. This correlation is expected, as shorter segment lengths result in more segments, and thus more places where protons interact with a neutrino beam reset to a narrow transverse width. Furthermore, the neutrino beam spread is smaller for shorter distances. However, the mechanical and engineering complexity of frequent beam bending and alignment limits how short the staggered segment lengths can be.

Figure 5 shows the dependence of the interaction rate on the pion beam RMS spot size on a log-log plot. An inverse power relation is observed for beam spot sizes above 1 mm. Beam spot sizes below 1 mm result in only minimal additional gain due to the inherent neutrino decay kinematic angle of $1/\gamma_\pi$, and the pion spread at decay caused by its transverse momentum.

4.3. Neutrino energies

Figure 6 shows the neutrino energy spectrum in the proton rest frame for neutrinos that cross the proton beamline. We find neutrino energies up to several hundred PeV, with the bulk of interactions in the tens of PeV range. The evolution of the average neutrino energy with distance along the proton beamline is illustrated in Figure 7, rising from about 150 PeV at the start to more than 300 PeV at the end of the beamline. This increase occurs because higher-energy pions, due to time dilation, have longer decay lengths, and thus are able to interact at greater distances.

Higher proton energies are expected to lead to increased event rates, as well as to larger average neutrino energies in the proton rest frame. Indeed, Figures 8 and 9 indicate that both approximately scale as the square of the proton energy.

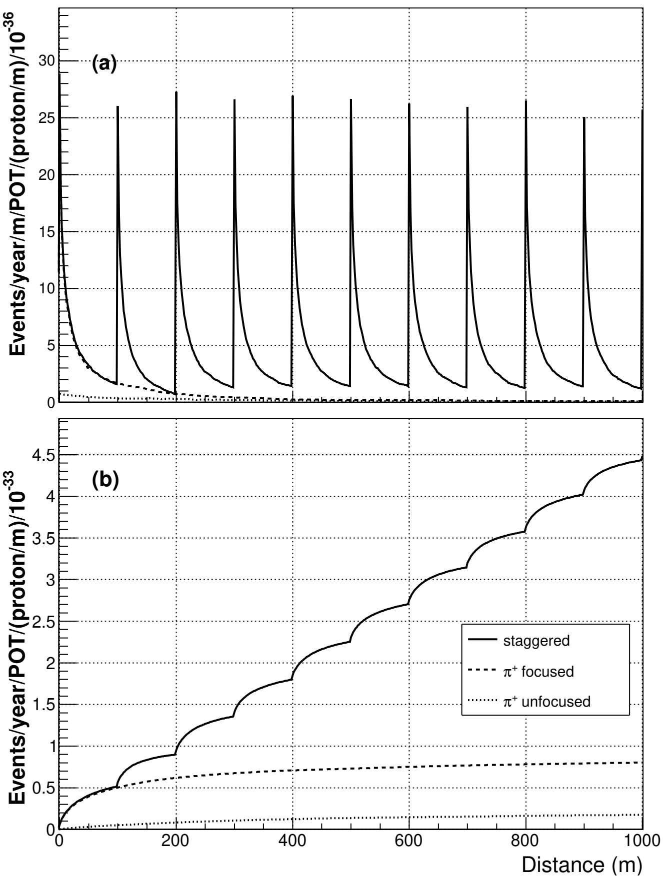

Figure 3: (a) Neutrino-proton events per meter vs. distance along the proton beam for three cases: focused pions with 1 mm RMS width and staggered beams; focused pions with beam dump; unfocused pions with beam dump. (b) Cumulative events for the same cases.

4.4. Contributions from muon decay

Including $\bar{\nu}_\mu$ from muons doubles the event rate compared to events with ν_μ from pions, with cooled muons leading to a fourfold increase.

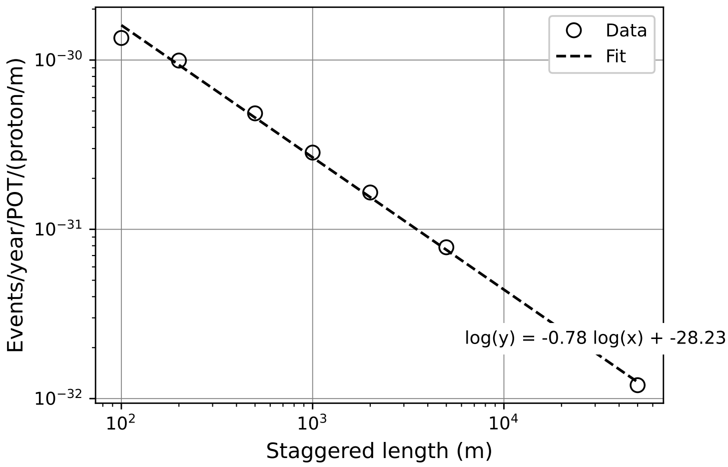

Figure 4: Log-log plot of neutrino-proton event rates versus staggered section lengths. Open circles represent simulation data, and the dashed line shows a linear fit in log-log space with the equation displayed.

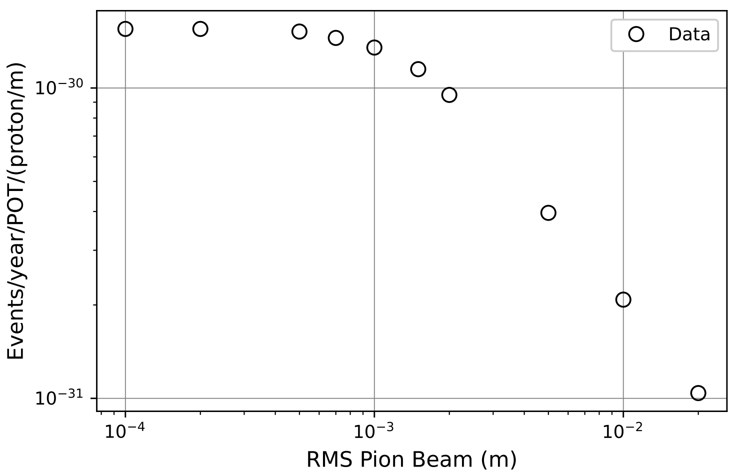

Figure 5: Log-log plot of neutrino-proton event rates versus RMS width of the pion beam. Open circles represent simulation data.

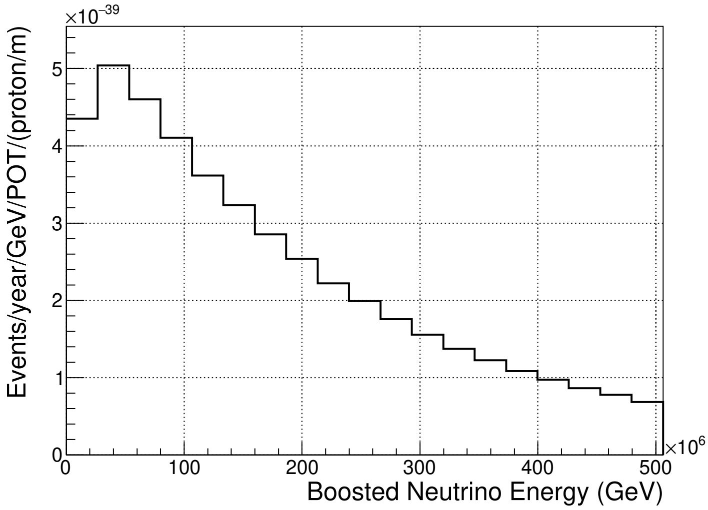

Figure 6: Neutrino energy distribution in the proton beam rest frame.

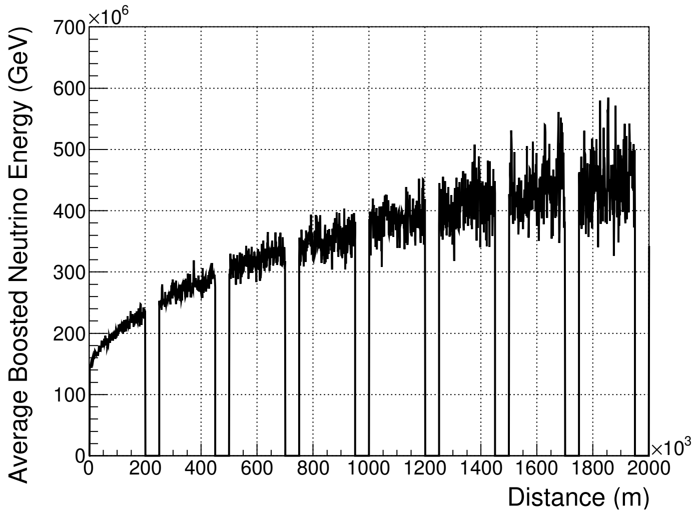

Figure 7: Average neutrino energy in the proton rest frame as a function of the distance from the target (including passing through multiple 200 km straight sections and 50 km intervening arcs).

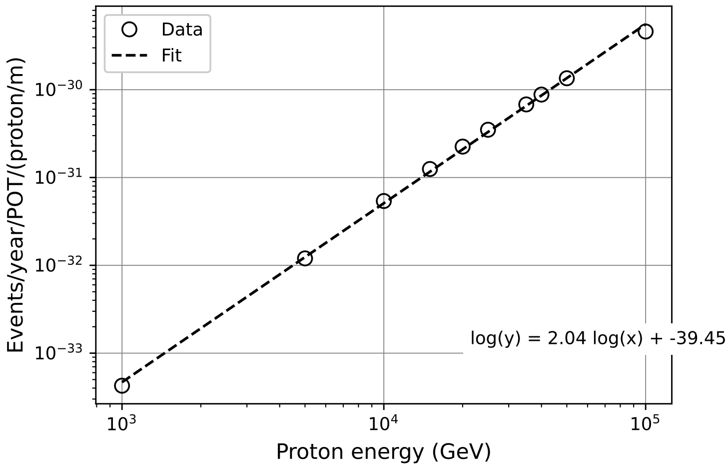

Figure 8: Log-log plot of neutrino-proton event rates versus proton energy (for protons impinging upon the proton target to produce pions, and for protons in the beamline). Open circles represent simulation data, and the dashed line shows a linear fit in log-log space with the equation displayed.

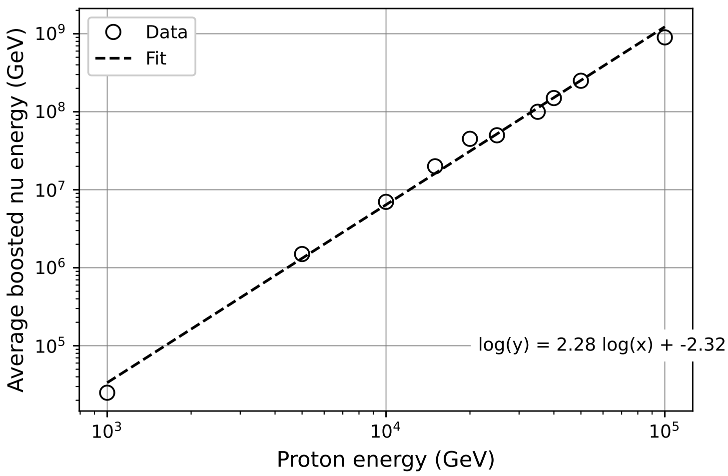

Figure 9: Log-log plot of the average boosted neutrino energy versus proton energy (for protons impinging upon the proton target to produce pions, and for protons in the beamline). Open circles represent simulation data, and the dashed line shows a linear fit in log-log space with the equation displayed.

4.5. *Final event rates*

Table 1 provides the number of neutrino-proton events per year and the average neutrino energy in the proton beam rest frame for three scenarios, based on FCC-hh Phase II parameters [20]. Final rates are found using Equation 2 and are given for neutrinos decaying from pions and from cooled muons.

The first scenario uses a 50 TeV proton energy. The current of the proton beam is set to $I = 0.5$ A, resulting in a proton line density $\lambda_p \approx 1 \times 10^{10}$ protons/m. The total number of protons in a beam is then $\approx 1 \times 10^{15}$. The minimum envisaged turnaround time at FCC-hh of $t_{\text{cycle}} \approx 1.8$ hours (including ramp-up, ramp-down, and fill time) is used to obtain $N_{\text{POT}}/\text{year} \approx 5 \times 10^{19}$. These calculations assume no downtime.

The FCC-hh has a current ceiling of 0.5 A due to large proton beam synchrotron radiation [20]. This limit prevents an increase in event rates through raising the current. However, synchrotron radiation power scales with energy as E^4, so, for example, a 20 TeV proton in an FCC-hh setup could instead have a 20 A current. The turnaround time could also shorten, as ramping magnets to 20 TeV is faster than to 50 TeV, to potentially about 1 hour per cycle instead of 1.8 hours (we use the FCC-hh fill time of 32 minutes and assume ramping times scale linearly with energy). This is the second scenario given in Table 1.

The third scenario is for a 10 TeV proton beam energy and again assumes that synchrotron radiation is the only limitation for the current and that ramping times scale linearly with energy.

Proton beam parameters			Neutrino-proton interaction rates and energies		
Proton energy (TeV)	Proton beam current (A)	Turnaround time (h)	ν_μ–p events/year	Cooled $\bar{\nu}_\mu$–p events/year	(Anti)Neutrino energy (p rest frame) (PeV)
50	0.5	1.8	0.7	3	250
20	20.	1.0	33.	130	45
10	312.	0.75	1500.	6000	7

Table 1: Neutrino-proton events per year using parameters based on the FCC-hh.

5. Discussion

The baseline scenario, using 50 TeV protons, yields an average neutrino energy in the proton rest frame of approximately 250 PeV, with event rates of about 0.7 neutrino-proton interactions per year, increasing to around 3 events with muon cooling. Although these rates are too small for detection, they are within a factor of ten to a hundred of being observable, indicating the potential viability of the staggered method for high-energy neutrino-proton studies.

In the 20 TeV proton scenario, the event rate improves significantly to approximately 30 events per year without cooling and over 100 with muon cooling, albeit at a reduced average neutrino energy of about 45 PeV. This trade-off between energy and event yield suggests that a 20 TeV setup could result in detectable rates at energies not achievable in any other foreseeable accelerator experiment.

Further reducing the proton energy to 10 TeV results in thousands of events per year, at energies of 5 to 10 PeV. Thus while the 50 TeV scenario does not result in detectable rates, the lower energy scenarios indicate that a good balance between energy and event yield can be achieved, particularly with the implementation of muon cooling.

These results demonstrate the potential of the proposed method to create a new energy frontier in neutrino physics, where controlled, high-energy neutrino-proton interactions can be measured.

6. Feasibility

The proposed method is extremely challenging from an engineering and accelerator design perspective, and very idealized assumptions were made in the simulation. Below are some of the issues and possible means of addressing them:

Pion beam focusing: In a typical neutrino accelerator experiment pions emerge from the production target and magnetic horn focusing system with a certain initial beam spot size (on the order of millimeters to centimeters [22]) and an inherent divergence due to their transverse momentum (p_T). In our scenario, we assume the pion beam can be focused to a small transverse size of about 1 mm and maintained at roughly that size throughout the decay channel. This might be achievable with a strong focusing lattice along the decay tunnel. High-energy pions experience less fractional deflection from a given p_T kick (since p_T/p_l is smaller at higher p_l), so focusing could be more manageable at multi-TeV momenta.

However, the large momentum spread would lead to chromatic effects, as lower-energy pions will diverge more between focusing elements than higher-energy ones. An achromatic design (perhaps pairing focusing and defocusing sections) might help, but beyond a certain momentum spread, it may not be possible to focus all pions equally well.

One possible mitigation is to keep only pions within a certain momentum range. Very low-energy pions (which would decay early anyway) and extremely high-energy pions (which might be too rigid to bend sufficiently in the staggered sections) could be removed. By reducing momentum spread, the focusing and bending challenges should become more tractable. Still, developing a lattice that can sustain a 1 mm beam over tens of kilometers will likely require new advances in magnet technology and beam dynamics.

A related issue concerns muon cooling. While the MICE collaboration demonstrated the principle of ionization cooling, it was performed at lower energies than those needed for our proposed concept.

Staggered bending sections: Each staggered segment end requires high-field bending magnets to offset the pion and proton beams in one direction and then return them. Pion beams, in particular, are challenging due to their momentum spread. Achromatic bending cells, with dipoles and quadrupoles arranged so that different momenta have converging trajectories, are needed to prevent emittance growth. Short, distributed bending, with many bending magnets to form a smooth trajectory rather than a sharp kink, might alleviate synchrotron radiation. A similar approach might be used to at least partially address the bending around the 50 km synchrotron arc, placing numerous achromatic bending sections with high-field magnets and applying extensive chromatic corrections.

Target: The high intensities and energies of the proton beams in the considered scenarios would destroy a stationary solid target. A solution could involve a moving or flowing target, such as liquid mercury [23].

Detector considerations: The muon path length at the considered TeV range of energies is several kilometers, and they will generally be at a very small angle with respect to the proton beam. One could thus envisage a series of muon trackers surrounding the proton beamline and placed every few hundred meters. If an extensive muon tracking system is installed along the beamline, the main background source would likely be proton beam–beam and beam–gas interactions creating showers with a high-energy muon.

Cost and complexity: The scale of the proposed setup, with hundreds of kilometers of staggered tunnels, likely thousands of magnets, a high-power target, and the requirement for very large currents, is beyond any current accelerator project and would depend on advances in accelerator technology and significant funding and energy commitments. This type of facility would combine elements of fixed-target neutrino production, which are known at moderate scales (meters to 100 m decay tunnels), with collider-scale beams and machine lengths (tens of kilometers), and with the need for extreme precision alignment (mm-level over km distances). Proton and muon colliders would likely need to be combined. Each aspect has been separately achieved to some extent, but not all together. Addressing these challenges would require a multi-stage R&D program, starting with scaled-down experiments at existing facilities to test the staggered beamline concept.

7. Conclusion

This paper presents a novel concept for a neutrino-proton collider experiment that could achieve interaction energies on the order of tens of PeV, significantly beyond the range of any existing or planned accelerator neutrino experiment.

Using a staggered beamline configuration and advanced beam-handling techniques such as muon cooling, the proposed method has the potential to reach the ultra-high-energy regime of astrophysical neutrinos. Simulations based on the FCC-hh parameters demonstrate that this approach could yield observable event rates in this energy range, with the potential for hundreds to thousands of interactions per year. Combining elements of a muon collider, in particular, could quadruple event rates.

Such a capability would provide measurements needed for models used in astrophysical neutrino observatories like IceCube and for exploring physics beyond the Standard Model at ultra-high energies. It would essentially extend the energy range of neutrino-proton fixed-target experiments by many orders of magnitude.

However, significant engineering challenges need to be addressed. Several requirements, such as the ability to maintain a narrow pion beam through hundreds of kilometers, are far beyond the current state of the art. Scaled down tests are needed before deciding whether the proposed method, or its possible variations, could become a viable technique to generate neutrino-proton events at the PeV scale and beyond.

8. Acknowledgment

This work was supported by the European Unions H2020 Spreading Excellence and Widening Participation - ERA Chair, grant agreement No 669014, and by the Ruder Boskovic Institute.

References

[1] L. A. Anchordoqui, et al., Cosmic neutrino pevatrons: a brand new pathway to astronomy, astrophysics, and particle physics, J. High Energy Astrophys. 1–2 (2014) 1–30. arXiv:1312.6587.
[2] K. Murase, R. Laha, S. Ando, M. Ahlers, Testing the dark matter scenario for pev neutrinos observed in icecube, Phys. Rev. Lett. 115 (2015) 071301. arXiv:1503.04663.
[3] J. Salvado, O. Mena, S. Palomares-Ruiz, N. Rius, Non-standard interactions with high-energy atmospheric neutrinos at icecube, J. High Energy Phys. 2017 (2017) 141. arXiv:1609.03450.
[4] Q. Wu, X. Xu, High-energy and ultra-high-energy neutrinos from primordial black holes, J. Cosmol. Astropart. Phys. (2025) 059arXiv:2409.09468.
[5] J. Salvado, O. Mena, S. Palomares-Ruiz, N. Rius, Neutrino interactions at ultrahigh energies, Phys. Rev. D 58 (1998) 093009. arXiv:hep-ph/9807264.
[6] A. Kusenko, T. J. Weiler, Interactions of high energy neutrinos, Phys. Rev. Lett. 88 (2002) 161101.
[7] A. V. Kisselev, V. A. Petrov, Gravireggeons in extra dimensions and interaction of ultra-high energy cosmic neutrinos with nucleons, Eur. Phys. J. C 36 (2004) 103.
[8] V. B. Valera, M. Bustamante, C. Glaser, The ultra-high-energy neutrino-nucleon cross section: measurement forecasts for an era of cosmic eev-neutrino discovery, J. High Energy Phys. (2022) 105.
[9] FASER Collaboration, First direct observation of collider neutrinos with faser at the lhc, Phys. Rev. Lett. 131 (2023) 031801.
[10] M. Aartsen, et al., Evidence for high-energy extraterrestrial neutrinos at the icecube detector, Science 342 (2013) 1242856.
[11] M. Aartsen, et al., First observation of pev-energy neutrinos with icecube, Phys. Rev. Lett. 111 (2013) 021103.
[12] M. Aartsen, et al., Observation of high-energy astrophysical neutrinos in three years of icecube data, Phys. Rev. Lett. 113 (2014) 101101.
[13] S. Aiello, et al., Observation of an ultra-high-energy cosmic neutrino with km3net, Nature 638, in press.
[14] V. Bertone, R. Gauld, J. Rojo, Neutrino telescopes as qcd microscopes, J. High Energy Phys. (2019) 217.
[15] J. A. Formaggio, G. P. Zeller, From ev to eev: neutrino cross sections across energy scales, Rev. Mod. Phys. 84 (2012) 1307.
[16] S. E. Kopp, Accelerator neutrino beams, Phys. Rep. 439 (2007) 101. arXiv:physics/0609129.
[17] A. Abada, et al., Fcc-hh: the hadron collider – future circular collider conceptual design report, Eur. Phys. J. Spec. Top. 228 (2019) 755–1107.
[18] MICE Collaboration, Demonstration of cooling by the muon ionization cooling experiment, Nature 578 (2020) 53–59.
[19] C. Accettura, et al., Towards a muon collider, Eur. Phys. J. C 83 (2023) 755.
[20] M. Benedikt, et al., Fcc-hh hadron collider – parameter scenarios and staging options, in: Proc. IPAC 2015, Richmond, VA, USA, 2015.
[21] T. Sjöstrand, et al., An introduction to pythia 8.2, Comput. Phys. Commun. 191 (2015) 159–177.
[22] J. Strait, et al., Long-baseline neutrino facility (lbnf) and deep underground neutrino experiment (dune) conceptual design report volume 3: Long-baseline neutrino facility for dune, Tech. rep. (2016). arXiv:1601.05823.
[23] H. G. Kirk, et al., The merit high-power target experiment at the cern ps, in: Proc. 11th European Particle Accelerator Conference (EPAC08), Genoa, Italy, 2008.